Water Research 212 (2022) 118116

Contents lists available at ScienceDirect

Water Research

journal homepage: www.elsevier.com/locate/watres

Spatiotemporal dynamics of microplastics in an urban river network area

Yifan Fan, Jinglan Zheng, Ligang Deng, Wenxin Rao, Qiji Zhang, Tong Liu *, Xin Qian *

State Key Laboratory of Pollution Control and Resources Reuse, School of the Environment, Nanjing University, 163 Xianlin Road, Nanjing 210023, China

ARTICLE INFO

Keywords:
Microplastics
Urban river network
Dynamics
Laser direct infrared

ABSTRACT

Microplastics contamination in the environment is a global problem, but little is known about their dynamics in urban river networks, an important site of microplastics occurrence and harboring complex transport pathways. In this study, we investigated the spatiotemporal dynamic of microplastics in a typical urban river network in eastern China from December 2018 to September 2019. microplastics abundance (mean ± standard deviation) in the river network ranged from 2.3 ± 1.2 to 104.6 ± 5.6 particles/L and was significantly higher during the wet than during the dry season. The distribution of microplastics in the upper, middle, and lower reaches of the river network did not significantly differ, nor did the abundance of microplastics in the surface water vs. the bottom water. However, high abundances were determined in commercial and industrial areas, at a wastewater treatment plant outlet, in an urban canal, and in an urban-rural fringe area. The seasonal dynamics of the overall abundance of microplastics could be explained by the hysteresis effect of urban plastic production and the variation in regional precipitation. 78.2% of the microplastics were < 330 μm in size; the most common colors were blue and black, and the most common shapes were fragments and fibers. The polymer types of the microplastics were assessed using laser direct infrared (LDIR), a novel chemical imaging system that identified silicone, rubber, polytetrafluoroethylene, and polypropylene as the main components of the microplastics. A non-metric multidimensional scaling analysis (NMDS) based on the abundance of the polymer components across samples showed aggregations of sampling sites, that indicated the possible sources of the microplastics. Our study provides insights into the spatiotemporal dynamics of microplastics in an urban river network and suggests the potential of LDIR in the accurate quantitative analysis of microplastics in the environment.

1. Introduction

As an emerging pollutant, microplastics (plastic particles < 5 mm in size) have raised global concern because of their ubiquity and potentially adverse effects on the environment (Browne et al., 2010; Sutherland et al., 2010; Thompson et al., 2004) and human health (Wu et al., 2019). An estimated 80% of the microplastic particles found in the world's oceans are discharged via rivers (Nocon et al., 2020), but the occurrence and transport of microplastics in freshwater ecosystems have not been well studied. Consequently, little is known about (1) the presence and distribution of microplastics in these systems and (2) the transport pathways and factors that affect microplastics distribution (Eerkes-Medrano et al., 2015).

Among the few studies of microplastics in freshwater systems, the majority have focused on large lakes and rivers whereas urban river networks have been largely ignored, in part due to their complex hydrology. However, because urban river networks are highly connected to the terrestrial environment, and thus to the sites of plastics production, use, and emission (Dikareva and Simon, 2019), they are important conduits of microplastics pollution.

Anthropogenic activities account for the generation and discharge of microplastics (Baensch-Baltruschat et al., 2020; Hernandez et al., 2017). In urban river networks, the presence of microplastics has been traced to household and industrial sewage discharge, the loss of feedstocks used to manufacture plastic products, and the breakdown of larger plastic items (Eerkes-Medrano et al., 2015). In addition, while nearly all microplastics entering municipal wastewater treatment plants (WWTPs) are removed from the influent, the load remaining in the effluent is still large enough to pose a threat to aquatic ecosystems and may account for a large share of the microplastics transported by urban rivers to downstream aquatic environments (Sun et al., 2019).

Studies on the temporal variation of microplastics in urban freshwater systems have been carried out in east Asia (Choong et al., 2021; Zhang et al., 2021), south Asia (Napper et al., 2021), Europe (de

* Corresponding authors.
E-mail addresses: liutong2018@nju.edu.cn (T. Liu), xqian@nju.edu.cn (X. Qian).

https://doi.org/10.1016/j.watres.2022.118116
Received 1 June 2021; Received in revised form 16 December 2021; Accepted 20 January 2022
Available online 24 January 2022
0043-1354/© 2022 Elsevier Ltd. All rights reserved.

Carvalho et al., 2021; Hurley et al., 2018), North America (Baldwin et al., 2016; Ballent et al., 2016), and Africa (Mbedzi et al., 2020). Nonetheless, there have been few long-term investigations, as such studies are both time-consuming and expensive. Moreover, due to differences in the sampling and detection methods used to assess microplastics in the environment, the comparability of the data is poor, including for urban freshwater systems. Given the importance of urban river networks in mediating the environmental distribution of microplastics, in this study, a typical urban river network in eastern China served as a model system for investigating the spatial and temporal dynamics of microplastics in riverine waters over a 1-year period.

The most common techniques used to study microplastics include stereomicroscopy for visual observation and Fourier transform infrared spectroscopy (FTIR) or Raman spectroscopy for polymer identification (Gong and Xie, 2020). Among the more recently developed methods used to identify the components of microplastics are pyrolysis gas chromatography-mass (Py-GC/MS) and focal plane array-based Fourier transform infrared (FPA-FTIR) imaging(Hendrickson et al., 2018; Ribeiro et al., 2020; Simon et al., 2018). Laser direct infrared (LDIR), a novel method for the automated detection of microplastics, was introduced in 2018 and has been applied in several studies of microplastics contamination in a groundwater aquifer (Samandra et al., 2022), at coastal sites (Scircle et al., 2020), in agricultural soil (Li et al., 2021), and in mammalian intestinal tissue (Li et al., 2021). Nonetheless, there are no published investigations of microplastics in the urban river network as determined using LDIR. In this study, we combined LDIR with a traditional microscopy exam in order to improve the accuracy and speed of detection of microplastics polymer types.

2. Methods and materials

2.1. Study area

The study site was the WangYu River network (Wuxi, China), the only diversion channel linking the Yangtze River, the largest river in China, and Taihu Lake, the third-largest freshwater lake in China. The river network has an area of ~500 km^2 and covers the main urban, urban-rural fringe, and rural areas of Wuxi City. Located on the Yangtze River delta, Wuxi is one of the most developed cities in China and its population density (> 2000 people/km^2 in 2017) is among the highest in the country. The Grand Canal, one of the busiest shipping channels in China, crosses the river network. Previous investigations of microplastics in the surface water of Taihu Lake using different sampling and extraction methods determined an abundance of 3.4–25.8 particles/L in August 2015 and 0.53 particles/L from August to September 2018. The microplastics levels measured in plankton net samples collected from Taihu Lake are among the highest reported in freshwater lakes worldwide (Li et al., 2019; Su et al., 2016). In the middle and lower reaches of the Yangtze River, the average abundance of microplastics from November to December 2017 was 4.92 $\times$ 10^5 particles/km^2 (Xiong et al., 2019).

2.2. Sample collection

The sampling sites and water flow are shown in Fig. 1. The 17 sampling sites consisted of 1 mainstream (WangYu River, sites WY-1–4), 2 primary tributaries (JiuLi River and BoDu River, sites JL-1–3 and BD-1–3), 2 secondary tributaries (sites JL-0 and BD-0), and 5 other representative sites: a commercial area (site C), an industrial area (site I), a wastewater treatment effluent outlet (site W), the Grand Canal (site JH), and a rural area (site R). The whole river network was divided into three parts according to its flows: the upstream sites C, JL-1, BD-1, and W; the midstream sites JL-0, JL-2, JL-3, BD-0, BD-2, BD-3, I, R, and JH; and the downstream sites WY-1–4.

Water samples were collected in December 2018 and in March, June, and September 2019, corresponding to winter, spring, summer, and autumn. 2 L of riverine surface water and 2 L of bottom water were collected from each of the 17 sites using a standard Rutter water sampler (Hydro-bios, Germany) and then transferred into purified glass bottles. In total, 136 water samples were finally collected. Water-quality indicators (total phosphorus, total nitrogen, chlorophyll-a, electrical conductivity, oxidation–reduction potential, dissolved oxygen, temperature, and turbidity) were measured simultaneously using a multi-parameter analyzer (LH-3BA, Lianhua Technology, China) and a portable multi-parameter water quality analyzer (AAQ-177, JFE Advantech, Japan). Local meteorological and air quality data were

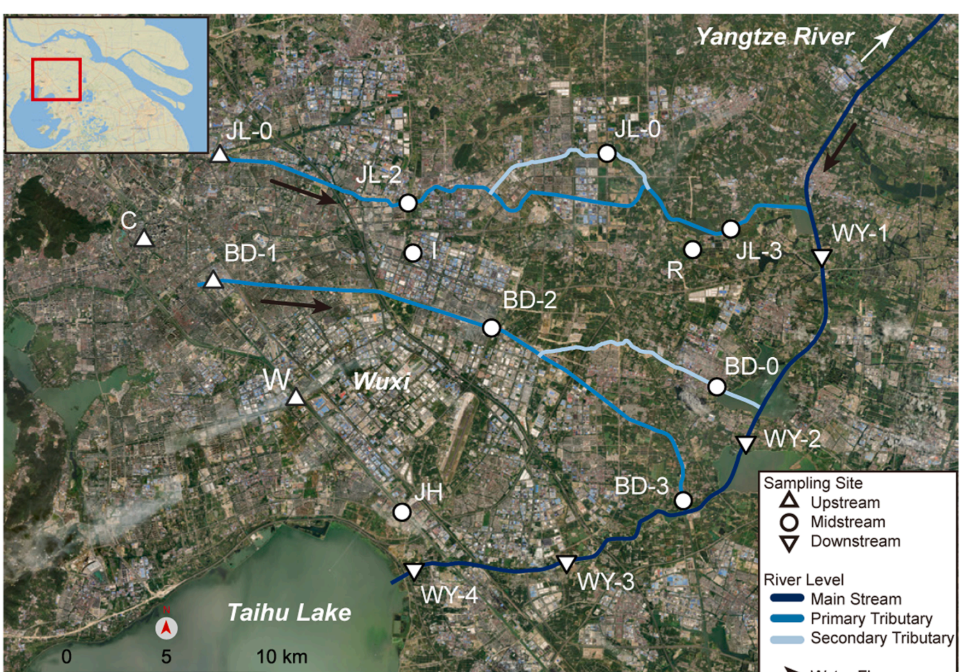

Fig. 1. Sampling sites of the WangYu River network area in Wuxi, China. The site abbreviatations are explained in the text.

acquired from a local meteorological station. Plastic industry data were obtained from the annual report of Wuxi City.

2.3. Microplastics extraction

Microplastics in the samples were extracted based on the protocol of the US NOAA (Masura, 2015), with slight modifications. In detail, 500 mL of a well-mixed water sample was transferred in triplicate to 500-mL glass beakers, which were then covered loosely with aluminum foil and placed in a 50 °C drying oven for 48 h. The dried samples were mixed with 20 mL of iron solution (Fe(II), 0.05 M) and 20 mL of 30% H_2O_2 and allowed to stand for 96 h with regular stirring to digest labile organic matter. The microplastics in the samples were obtained by density separation in $ZnCl_2$ solution ($\rho = 1.7$–1.8 g/mL). The floating layer was filtered onto a polycarbonate filter (5 μm, Ø 47 mm, Millipore) using a vacuum pump. The filter was covered with a clean glass petri dish and air-dried for 24 h. The extracted microplastics were then examined using a stereomicroscope (MZ62; Guangzhou Mshot Photoelectric Technology, China) and their size (maximum length in one-dimension), shape, and color were recorded.

2.4. Polymer composition identification

LDIR is a novel and automated approach to identifying the polymer types in microplastics. It is less labor-intensive than FTIR and Raman spectroscopy but its accuracy and efficiency in component detection are higher than either of these traditional methods. Nonetheless, to reduce the time and economic costs associated with the analysis, five key sites (sites C, I, W, WY-1, and WY-4) from the 17 sites included in the study were selected to identify the polymer composition of the collected microplastics using LDIR.

For each sample, a 10-mm × 10-mm square was cut from each filter using a stainless-steel blade and then transferred into a 1.5-mL glass crimp top vial (PerkinElmer, USA). The triplicate samples were pooled, such that the four sampling periods and the two positions of the water column (surface and bottom) from the five sites resulted in 40 samples in total. The samples were preserved by the addition of 0.2 mL of absolute ethyl alcohol and then analyzed in an LDIR automatic chemical imaging system (8700 LDIR, Agilent, USA). The polymer types of the samples were identified using attenuated total reflectance (ATR) mode; the threshold quality for polymer identification was set to > 0.7.

2.5. Quality control and blank test

Quality control was run throughout the sampling, extraction, and identification of microplastics. People handling the samples wore cotton lab coats and natural latex gloves at all times. All instruments and containers used at each step were of stainless steel or glass and were rinsed three times with pre-filtered Milli-Q water (0.45-μm GF/F filter paper, Ø 47 mm). All solutions, including $ZnCl_2$ and Fe(II) solutions, were prepared using the pre-filtered Milli-Q water. The laboratory experiment was conducted in a fume hood. All open containers were covered with aluminum foil to avoid contamination with microplastics pollution from the air.

Triplicate procedural blanks were run, from the field sampling to microplastics extraction, using the pre-filtered Milli-Q water as the blank control of the water samples. A plastic-like fiber (482 μm in size) trapped on the filter and was identified as a natural fiber using a μ-FT-IR microscope (Hyperion 2000, Bruker, Germany). Accordingly, the detection limit of the extraction procedure was set as 0.7 particles/L, and the actual sample results were corrected for the blank value. Recovery experiments, using standard microplastics as samples, were also carried out. The lowest quantity recovery rate was 90% (Table S1), and the lowest mass recovery rate was 87% (Table S2).

2.6. Statistical analyses

The data were recorded using Microsoft Excel and then analyzed using R ver. 3.6.2. Kruskal-Wallis and Mann-Whitney U tests were used to compare the temporal and spatial differences in the mean abundance of microplastics ($\alpha = 0.05$). QGIS ver. 3.10 was used in the cartographic visualization. The LDIR data were subjected to non-metric multidimensional scaling (NMDS) to explore the transport behavior of microplastics in the urban river network. Distances were sorted using a Bray-Curtis distance analysis. Two sort axes were defined to obtain the iteration results. The stress value and a Shepard plot were used to evaluate the results of the NMDS analysis.

3. Results

3.1. Morphological description of microplastics

In total, 7763 microplastics were observed by stereomicroscopy (Fig. 2). Their morphologies are summarized in Fig. 3. Fragments (52.4%) and fibers (32.5%) were the most common shapes (Fig. 3A), and blue (60.5%), red (10.9%), and black (10.6%) the most common colors (Fig. 3B). Specifically, the majority of the microplastics consisted of blue fibers and blue and red fragments (Fig. 3C). Most (78.2%) of the microplastics were < 330 μm, a size commonly obtained in manta trawls. The median and mean sizes were 98 and 275.9 μm, respectively. The size and shape distribution followed similar patterns, whereas a comparison of the combined size and color distribution showed a smoother distribution of fibers than of other shapes. The median and mean sizes of particles other than fibers were 73 and 112 μm, respectively ($n = 5237$), with 95.1% of them < 330 μm in size. Thus, as proposed in previous studies, fibers can be regarded independently as "microfibers" (Sait et al., 2020). Neither a power-law distribution nor a logarithmic normal distribution was applicable to the size distribution of the microplastics in this study (Kolmogorov-Smirnov test, $p < 0.05$).

3.2. Spatiotemporal abundance of microplastics

The spatial abundances of microplastics in the surface and bottom waters from the sample sites across the four seasons are shown in Fig. 4A. In the surface-water samples, the highest mean abundance of microplastics (159.3 particles/L) was detected at site JH in summer whereas no microplastics were detected in the triplicate samples from site JL-0 and site WY-3 in spring. In the bottom-water samples, microplastics abundance reached 193.3 particles/L at site JL-0 in autumn, whereas no microplastics were detected at site JL-3 in winter, site BD-1 in spring, site I in spring, and site JL-1 in summer.

The seasonal dynamics of microplastics abundance differed significantly between spring and summer in the water column as a whole and in all areas except the upstream bottom water (Mann-Whitney U test, $p < 0.05$). The mean abundance of microplastics was significantly higher during the wet season (Jun 2019 and Sept 2019) than during the dry season (Dec 2018 and Mar 2019).

The spatial distribution of microplastics across the year did not significantly differ, as there were no significant differences between the upstream, midstream, and downstream areas nor between the surface and bottom waters, except the vertical difference in March 2019 (Fig. 4B). From December 2018 to September 2019 the microplastics abundance (mean ± standard deviation) for the up-, mid-, and downstream of the river network ranged from 2.3 ± 1.2 to 104.6 ± 5.6 particles/L.

As anthropogenic pollutants, microplastics are fundamentally derived from plastic products, including the emission of primary microplastics (Wang et al., 2019). We therefore compared the quarterly accumulated growth rate of plastics products output in Wuxi City and the seasonal average microplastics abundance in the river network via 0–1 normalization (Fig. 5). The accumulated growth rate of plastics

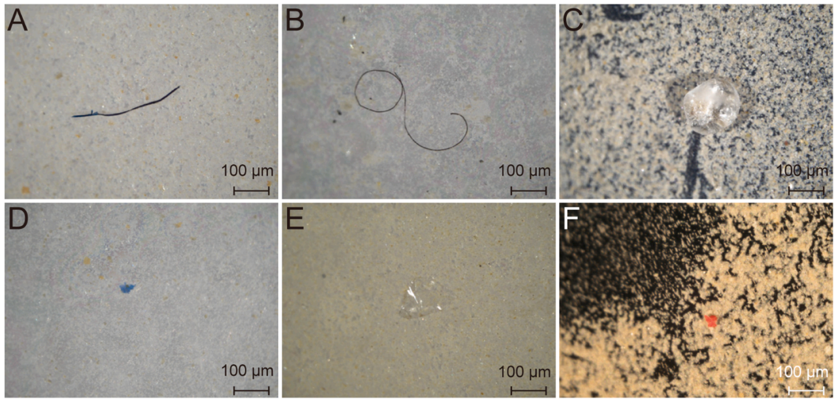

Fig. 2. Microplastics as seen using stereomicroscopy. The photographs show (A) a blue fiber, (B) a black fiber, (C) a transparent pelletm, (D) a blue fragment, (E) a transparent film, and (F) a red fragment (For interpretation of the references to color in this figure legend, the reader is referred to the web version of this article.).

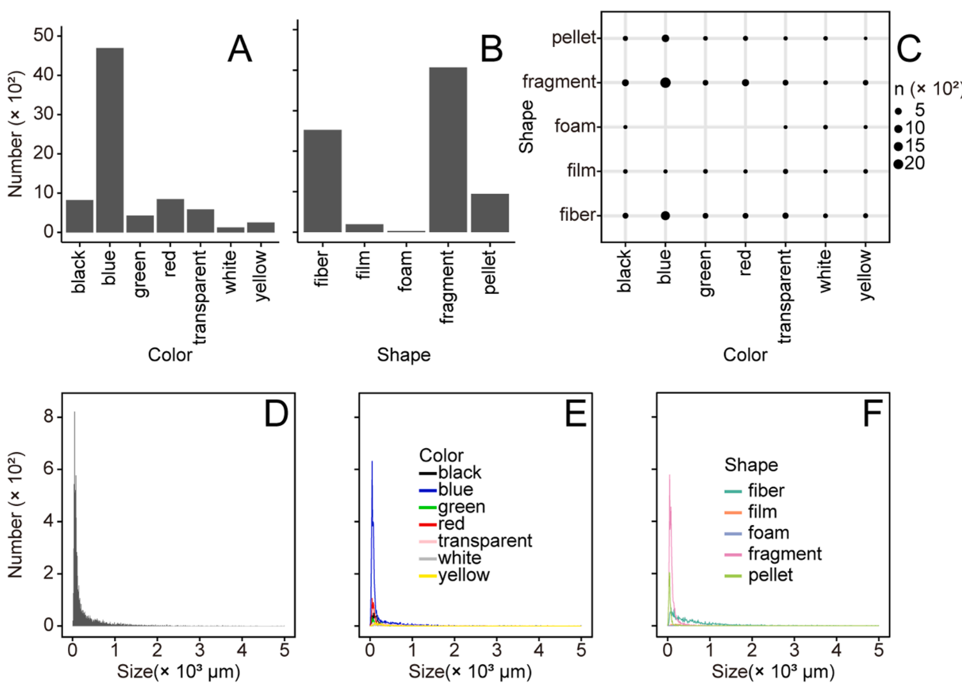

Fig. 3. Summary of the morphology of the detected microplastics. (A) Frequency of colors, (B) shapes, and (C) combinations thereof in the collected microplastics. (D) Global size distribution and the size distribution based on the color (E), and shape (F) of the collected microplastics (bandwidth = 10 μm).

products output significantly increased during the first quarter of 2019 (22.7%), such that the mean abundance of microplastics correspondingly peaked in June 2019 (2019 Q2; 104.6 particles/L). The curves of both normalized indexes indicated a “hysteresis effect” (Fig. 5, black arrow). Another factor potentially affecting the abundance of microplastics in the riverine water is the variation in the amount of regional precipitation (Fig. 5, blue line). Increased surface runoff due to precipitation may carry microplastics from the atmosphere and from terrestrial systems into rivers (Grbic et al., 2020; Klein and Fischer, 2019; Wong et al., 2020; Zhou et al., 2021). In this study, the abundance of microplastics in the wet season (June 2019 and September 2019) was significantly higher than during in the dry season (December 2018 and March 2019), thus correlating positively with the regional accumulated daily precipitation. However, the region experienced a heavy rainstorm in August 2019 (113.6 mm), which may have diluted the concentration of microplastics in the river, resulting in a drop in the average abundance of microplastics in September 2019 compared with the previous season. In summary, seasonal differences in microplastics abundance in the studied urban river network could be explained by urban plastic production and regional precipitation.

3.3. *Polymer composition of the microplastics*

LDIR identified 22 polymer types in the microplastics samples (Fig. 6). With respect to the proportion of polymer types, the seasonal, spatial, and vertical distributions were roughly similar and stable, with silicone, polytetrafluoroethylene (PTFE), and rubber as the most abundant polymer types by number concentration. Previous studies on microplastics in other urban water bodies mainly detected polypropylene (PP), polyethylene (PE), polystyrene (PS), and polyethylene terephthalate (PET) (Bujaczek et al., 2021; Peng et al., 2018; Wang et al., 2020). The corresponding abundances were calculated based on the proportion of the polymer compositions of each sample. As shown in Fig. 6C, the industrial area (site I) continuously contributed PTFE microplastics, and rubber microplastics were mainly emitted in June 2019. Our findings thus provide information on the nature of microplastics pollution in the study area.

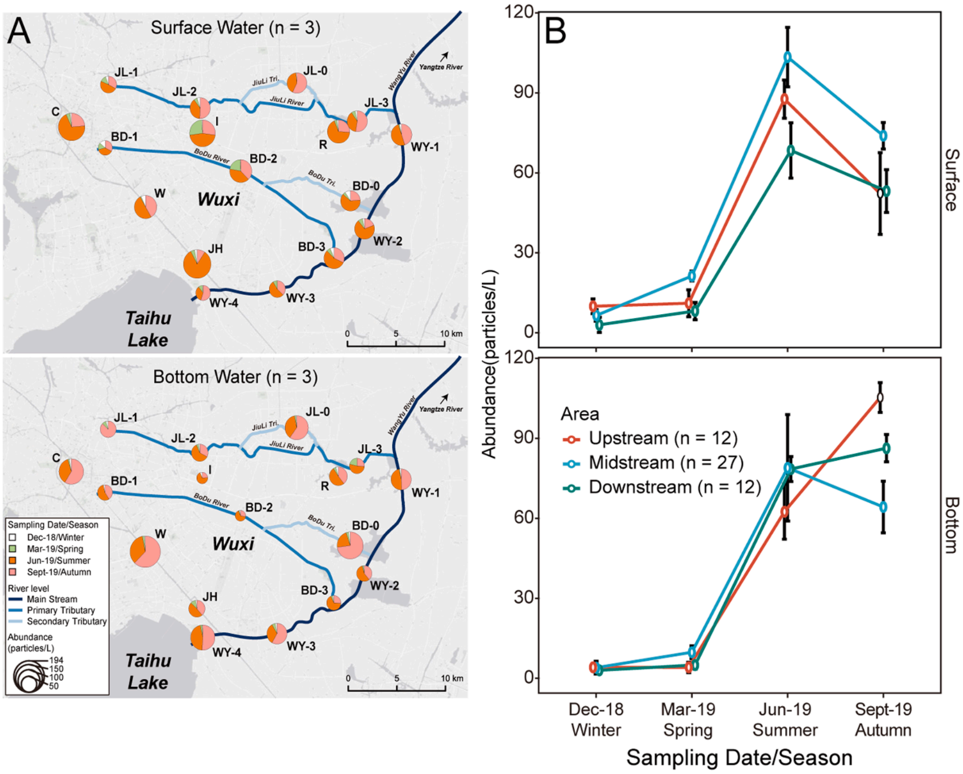

Fig. 4. Spatiotemporal dynamics of the microplastics in the WangYu River network area from December 2018 to September 2019. (A) Mean abundance of microplastics in the surface water (upper panel) and bottom water (lower panel) across the four seasons. (B) Temporal distribution of microplastics according to their up-, mid-, and downstream locations and their vertical position in the water columns (upper panel: surface water, lower panel: bottom water). The datapoints were adjusted to improve clarity. The error bars represent the standard deviation (sd).

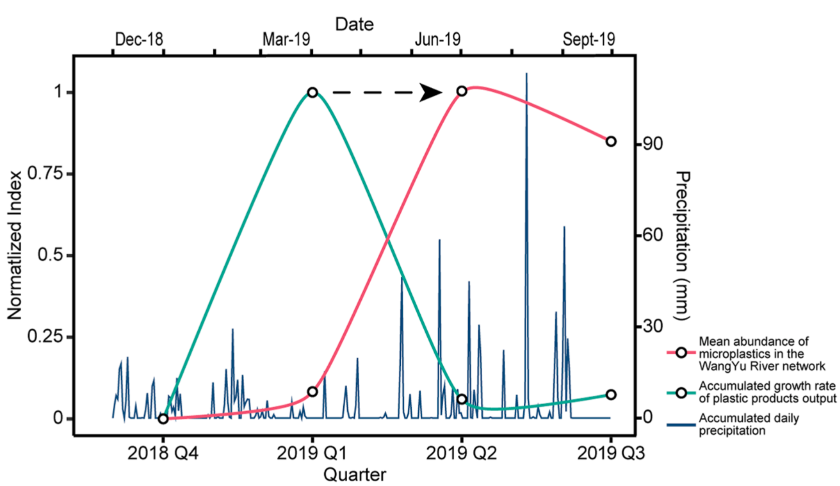

Fig. 5. Normalized index (NI) of the accumulated growth rate of plastic products output of Wuxi City (green curve) and the mean abundance of microplastics in the WangYu River network (red curve) from 2018 Q4 (December 2018) to 2019 Q3 (September 2019). The accumulated daily precipitation of Wuxi City from December 1, 2018 to September 30, 2019 is shown in blue (For interpretation of the references to color in this figure legend, the reader is referred to the web version of this article.).

3.4. NMDS analysis

Data standardization following the LDIR analysis was not possible due to the small number of microplastics detected in a single sample and the large differences in the quantities of the detected components. Instead, the frequency of every microplastics component identified in the samples collected at each site across the four seasons was determined, with the microplastics abundance data then subjected to an NMDS analysis. The results are shown in Fig. 7. The resulting NMDS models were evaluated using a Shepard plot and based on the stress value, which indicated that the models were reasonable (Fig. S1). The analysis based on the abundances of the polymer components revealed that the data from the ten sampling points could be aggregated into four categories (Fig. 7, black circles).

4. Discussion

4.1. Spatiotemporal dynamics of microplastics

High levels of microplastics pollution have been reported in the urban river networks of several countries (Table 1). In China, microplastics pollution in urban rivers can be explained by the fact that urban areas themselves are heavily polluted by microplastics (Wang et al., 2019). In our study, the abundances of riverine microplastics in June 2019 and September 2019 (wet season) were 1–2 orders of magnitudes higher than in December 2018 and March 2019 (dry season), a pattern was also observed in other temporal investigations (Eo et al., 2019; Rodrigues et al., 2018). Our study demonstrated that, in the urban river network, the temporal variation of microplastics abundance in riverine water could be attributed to the combined effect of the temporal variation in regional precipitation and urban plastic production.

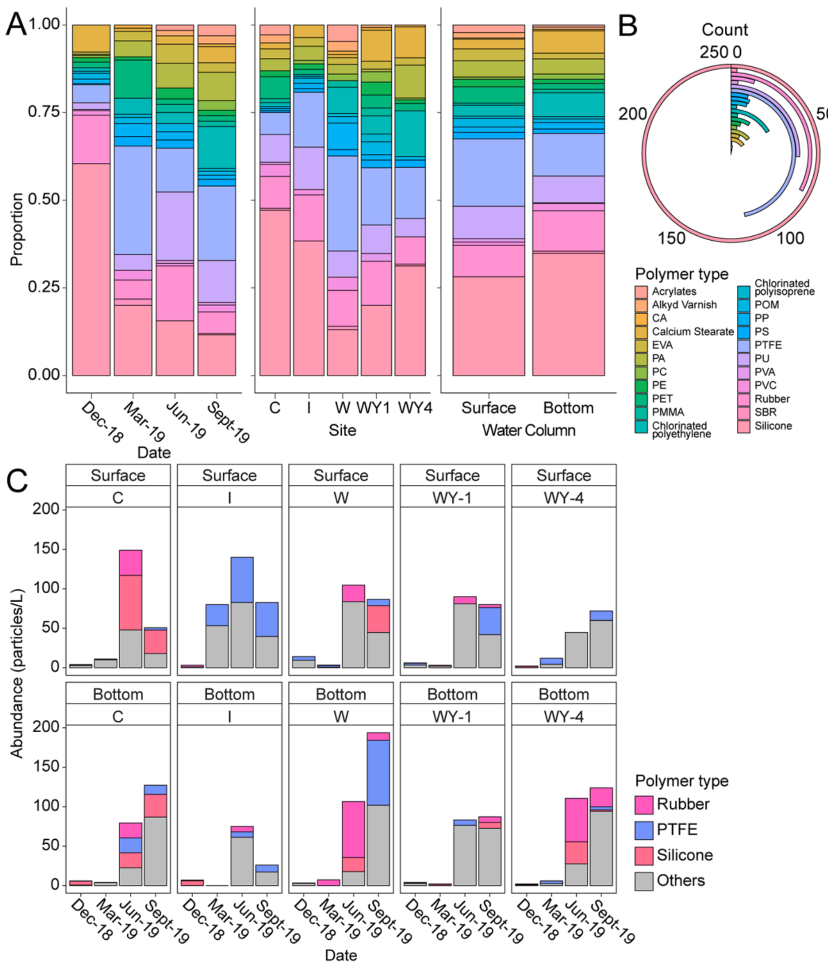

Fig. 6. The spatiotemporal occurrence of different microplastics' polymer types determined by LDIR and stereomicroscopy. (A) The temporal, spatial, and vertical propotions of all identified polymer types. (B) The count of all identified polymer types. (C) The corresponding abundance of the three most abundant (by number) polymer types (silicone, PTFE, and rubber); the other polymer types are shown in gray.

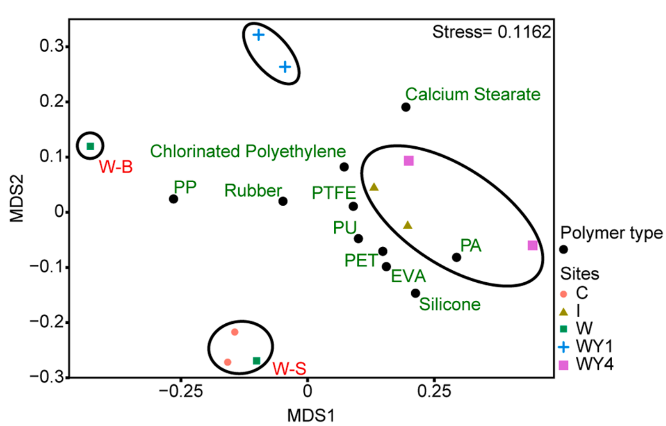

Fig. 7. NMDS analysis of microplastics composition abundance. The polymer type in the microplastics is shown in green, and the sampling site in red (S: surface water, B: bottom water). The 10 most abundant components by numberare are shown. The black circles indicate the aggregations of the sampling points (For interpretation of the references to color in this figure legend, the reader is referred to the web version of this article.).

The spatial distribution of microplastics abundance reflected the differences in the microplastics burden across the sampling sites. The commercial area (site C) has the highest population density in the river network area, which accounted for the high level of microplastics

Table 1
Published data on microplastics abundance in riverine surface waters.

Location	Sampling date	Mesh size (μm)	Mean abundance of microplastics (particles/L)	Refs.
Gallatin River watershed, USA	Sept 2015–Jun 2017	0.45	1.2	(Barrows et al., 2018)
Antuã River, Portugal	Mar and Oct 2016	55	0.058–1.265	(Rodrigues et al., 2018)
Guangzhou, China	Jul 2017	20	0.379–7.924	(Lin et al., 2018)
Nakdong Riber, South Korea	Oct 2017	20	0.293–4.76	(Eo et al., 2019)
The Netherlands	Autumn 2017	20	0.067–11.532	(Mintenig et al., 2020)
Yulin River, China	Jan 2018	64	0.013–0.36	(Mao et al., 2020)
Shanghai, China	Summer and winter 2018	80	14.4–26.2	(Chen et al., 2020)
Lijiang River, China	Jul 2019	75	0.0675	(Zhang et al., 2021)
Siberia, Russia	Jun 2020	330	0.0442–0.0512	(Frank et al., 2021)
Wuxi, China	Dec 2018–Sept 2019	5	2.3–104.6	This study

The data were obtained in a literature search in the Web of Science.

occurrence at this site. At the WWTP effluent outlet (site W) and the canal (site JH), large-volume inflows of plastics together with a busy waterway (Carr et al., 2016; Leslie et al., 2017) located in the midstream of the river network results in high abundances of microplastics. At the urban-rural fringe area (site JL-0 and BD-0), the population size is relatively small, but poor environmental management may be responsible for the high level of microplastics contamination.

In the industrial area (site I), the abundance of microplastics in the water column was highly stratified (Fig. 4), with high abundances in the surface water and low abundances in the bottom water. This may reflect the placement of an effluent outlet near the surface of the water column (Fig. S2), a common practice of the area's factories. Furthermore, the high water flow velocity of these outlets causes microplastics within the effluent to be transported downstream before sinking. However, differences in the abundance of microplastics throughout the water column of the urban river network area were only slightly significant (Fig. 6), thus illustrating the complex vertical distribution of microplastics in river waters.

4.2. Compositions and transport behavior of microplastics in an urban river network

We used a novel detection method (LDIR) to identify and semi-quantify microplastics in the urban river network. The Agilent 8700 LDIR chemical imaging system uses a Quantum Cascade Laser (QCL) combined with a point detector and rapidly scanning optics. The instrument can automatically obtain a microparticle's IR spectrum, identify its polymer type within 8 s, and generate a report (Fig. S3). Currently, only four studies have been reported in which LDIR was used to analyze microplastics: in soil ($n = 34$) (Li et al., 2021), coastal water ($n = 20$) (Scircle et al., 2020), groundwater ($n = 21$) (Samandra et al., 2022), and animal intestinal tissue ($n = 3$) (Hua et al., 2021). Therefore, this study may be the first to employ LDIR to analyze microplastics in river water, and the sample scale was the largest ($n = 40$ in LDIR workflow).

In this study, 808 microplastics were detected and identified using LDIR compared with 2782 determined using stereomicroscopy. Since the filter area used in the LDIR detection (10 mm $\times$ 10 mm) accounted for only 8% of the whole filter (Ø 47 mm), the abundance of microplastics determined by LDIR may have been 3.63 times higher than determined by the traditional stereomicroscopy exam. As this was a pilot study of a novel detection method, the abundance of microplastics was also determined visually. In the future, LDIR analysis workflow may become the preferred mode of analysis of microplastics polymer type and abundance in the environment.

The most abundant polymer types (silicone and PTFE) detected in the microplastics analyzed in this study were less commonly identified in similar studies using FTIR or Raman spectroscopy in polymer identification, in which the ranking was PE $\approx$ PP $>$ PS (Klein et al., 2015; Koelmans et al., 2019; Lin et al., 2018; Mintenig et al., 2020; Wang et al., 2020). Silicone is a common component of personal care products, cookware, and other consumer goods and has been detected in the effluents of WWTPs, including in a large North American city (Grbic et al., 2020). PTFE is widely used in electrical appliances, machinery, and many industrial applications due to its excellent corrosion resistance, but it has a long half-life in the environment. Moreover, PTFE is a class 3 carcinogen, although its effects on human and aquatic ecosystems are poorly understood. PTFE cannot be detected by FTIR (Mani et al., 2019), but it can be detected by LDIR, which showed that it was the second most abundant polymer in the WWTP effluent. Thus, PTFE contamination in the environment should be regularly assessed using the appropriate detection methods.

Other parameters of the microplastics were also assessed, including polymer abundance and area, both of which could be estimated using the LDIR data (Fig. S4). In terms of the surface area of the particles, silicone, rubber, PP, PTFE, polyethylene terephthalate (PET), and PE were the predominant polymer types (Table S3). Relatively high abundances and areas were determined for silicone, PTFE, and rubber, consistent with their being the main components of microplastics in the studied urban river network. PP and PE ranked 2nd and 6th in polymer area, respectively, but their low abundances suggested that the individual PP or PE microplastic particles in the samples were larger, allowing them to be readily detected using traditional methods based on manual sorting (i.e., visual observation and FTIR/Raman spectroscopy).

According to the NMDS analysis (Fig. 7), the coordinate distances of the surface water and bottom water at the same sampling site were close. The exception was the WWTP sites (W-S and W-B), which indicated that the microplastics composition in the water column at these sites was mostly homogeneous. Since the effluent outlet of the WWTP was located near the surface of the water column (Fig. S5), water samples from sampling point W-S consisted mainly of WWTP effluent. Samples from the commercial area (C-S, C-B) and W-S were classified within the same group but were separated from the bottom water of the WWTP (W-B), indicating that microplastics in the WWTP effluent mainly derived from the urban commercial area. The aggregation of samples from the industrial area (I-S, I-B) with those obtained downstream in the WangYu River (WY-4-S, WY-4-B) suggested that microplastics in the latter were mainly industrial in their origin. Calcium stearate, chlorinated polyethylene, PTFE, PU, PET, chlorinated polyethylene, EVA, silicone, and PA were the main polymer types. The WY-4 site was located at the entrance of the WangYu River's mainstream, towards Taihu Lake. Thus, according to the NMDS analysis, the largest source of microplastics flowing into Taihu Lake via the river network is the industrial area.

4.3. Microplastics contamination from the WWTP effluent

Given the critical role of the WWTP in releasing microplastics into the river network, the microplastics in its WWTP effluent were examined in greater detail. The W-S sampling site represented the effluent outlet of one of the largest WWTPs in Wuxi City. Microplastics in the surface water from this site were mostly blue and red fragments and fibers. The mean annual abundance of microplastics was 52.2 particles/L. Among the 14 polymer types identified in the respective samples by LDIR, silicone, PTFE, and polyurethane (PU) made up the largest share. As PU is mainly used as foams, elastomers, and fibers but it is also a component of paint chips, such that paint spalling may have accounted for the PU microplastics in the samples (Corcoran et al., 2020). PU monomers have been classified as carcinogenic, mutagenic, or both, their environmental and health effects have raised serious concern (Wright and Kelly, 2017).

The shapes and colors of microplastics in the WWTP effluents analyzed in studies conducted in other regions were similar to those in our study, whereas the polymer types identified using traditional methods differed (Table 2). Raman spectroscopy and FTIR of those WWTP effluent samples mostly identified PP and PE, while the components detected by FPA-FTIR were diverse. Our analysis using LDIR demonstrated that 1) microplastics in WWTP effluents differ in their spatial distribution and their source and 2) there is a need for unified and standardized methods of microplastics analysis to allow comparisons of the results of different studies.

5. Conclusions

Our investigation of the spatiotemporal dynamics of microplastics in a typical urban river network in China revealed a strong temporal variability in terms of the abundance of microplastics at the different sampling sites. The high abundances during the wet season and low abundances during the dry season could be explained by the hysteresis effect of urban plastic production, and the variation in regional precipitation. The smooth spatial variability of microplastics abundance, both longitudinally and vertically, was demonstrated as well. According to the LDIR analysis, the predominant polymer types in the microplastics isolated from the urban river network were silicone, PTFE, rubber, and

Table 2
Published information on microplastics in the effluents of domestic WWTPs.

Location	Mesh size (μm)	Detection method	Microplastics abundance (particles/L)	Main colors	Main shapes	Main polymer types	Refs.
Changzhou, China	13	Visual observation /Raman	6–40	transparent, white	fragment, film	PE, PP, PS	(Wang et al., 2020)
Wuhan, China	14.9	Visual observation /Raman	7.9–80.5	transparent	fiber, fragment, microbead	PVC, PE, PP	(Tang et al., 2020)
South Korea	45	Visual observation /FTIR	0.004–0.51		fragment	PP, PE, PET	(Park et al., 2020)
Xiamen, China	43	Visual observation /Raman	0.20–1.73	white, transparent	granules, fragments, fibers, pellet	PE, PP, PE-PP	(Long et al., 2019)
Denmark	10	FPA-FTIR	19–447			PE, PE-PP, acrylate	(Simon et al., 2018)
Lower Saxony, Germany	20	FPA-FTIR	0.001–9.005		particulate, fiber	PP, PE, PA, styrene acrylonitrile (SAN)	(Mintenig et al., 2017)
The Netherlands	0.7	Visual observation/ FTIR	51–81				(Leslie et al., 2017)
Scotland	65	FTIR	0.25	red, blue, green	flake, fiber, film	Polyester, PA, PP	(Murphy et al., 2016)
Wuxi, China	5	Visual observation/ LDIR	52.2	blue, red	fragment, fiber	silicone, PTFE, PU	This study

FTIR: Fourier transform infrared spectroscopy, FPA-FTIR: Focal plane array Fourier transform infrared spectroscopy, -: not available.
The data were obtained in a literature search in the Web of Science.

PP, but other unusual polymer types were identified as well. In the WWTP effluent, LIDR detected silicone, PTFE, and PU as the major components of the microplastics. An NMDS analysis based on the abundances of microplastic polymer types suggested that microplastics released in the commercial area were mainly transported to the WWTP, and microplastics from the industrial area mainly to the mainstream of the river network. The process used in our analysis suggests a new approach to the study of the transport behavior of microplastics in freshwater systems.

Declaration of Competing Interest

The authors declare that they have no known competing financial interests or personal relationships that could have appeared to influence the work reported in this paper.

Acknowledgements

This study was supported by National Natural Science Foundation of China (No. 41907388).

Supplementary materials

Supplementary material associated with this article can be found, in the online version, at doi:10.1016/j.watres.2022.118116.

References

Baensch-Baltruschat, B., Kocher, B., Stock, F., Reifferscheid, G., 2020. Tyre and road wear particles (TRWP)-a review of generation, properties, emissions, human health risk, ecotoxicity, and fate in the environment. Sci. Total Environ. 733, 137823–137825.
Baldwin, A.K., Corsi, S.R., Mason, S.A, 2016. Plastic debris in 29 great lakes tributaries: relations to watershed attributes and hydrology. Environ. Sci. Technol. 50 (19), 10377–10385.
Ballent, A., Corcoran, P.L., Madden, O., Helm, P.A., Longstaffe, F.J, 2016. Sources and sinks of microplastics in Canadian Lake Ontario nearshore, tributary and beach sediments. Mar. Pollut. Bull. 110 (1), 383–395.
Barrows, A.P.W., Christiansen, K.S., Bode, E.T., Hoellein, T.J., 2018. A watershed-scale, citizen science approach to quantifying microplastic concentration in a mixed land-use river. Water Research 147, 382–392.
Browne, M.A., Galloway, T.S., Thompson, R.C, 2010. Spatial patterns of plastic debris along estuarine shorelines. Environ. Sci. Technol. 44 (9), 3404–3409.
Bujaczek, T., Kolter, S., Locky, D., Ross, M.S, 2021. Characterization of microplastics and anthropogenic fibers in surface waters of the North Saskatchewan River, Alberta, Canada. Facets 6, 26–43.
Carr, S.A., Liu, J., Tesoro, A.G, 2016. Transport and fate of microplastic particles in wastewater treatment plants. Water Res. 91, 174–182.
Chen, H., Jia, Q., Zhao, X., Li, L., Nie, Y., Liu, H., Ye, J., 2020. The occurrence of microplastics in water bodies in urban agglomerations: Impacts of drainage system overflow in wet weather, catchment land-uses, and environmental management practices. Water research 183, 116073–116073.
Choong, W.S., Hadibarata, T., Tang, D.K.H, 2021. Abundance and distribution of microplastics in the water and riverbank sediment in Malaysia-a review. Biointerface Res. Appl. Chem. 11 (4), 11700–11712.
Corcoran, P.L., Belontz, S.L., Ryan, K., Walzak, M.J, 2020. Factors controlling the distribution of microplastic particles in benthic sediment of the Thames River, Canada. Environ. Sci. Technol. 54 (2), 818–825.
de Carvalho, A.R., Garcia, F., Riem-Galliano, L., Tudesque, L., Albignac, M., Ter Halle, A., Cucherousset, J., 2021. Urbanization and hydrological conditions drive the spatial and temporal variability of microplastic pollution in the Garonne River. Sci. Total Environ. 769, 144479–144480.
Dikareva, N., Simon, K.S, 2019. Microplastic pollution in streams spanning an urbanisation gradient. Environ. Pollut. 250, 292–299.
Eerkes-Medrano, D., Thompson, R.C., Aldridge, D.C, 2015. Microplastics in freshwater systems: a review of the emerging threats, identification of knowledge gaps and prioritisation of research needs. Water Res. 75, 63–82.
Eo, S., Hong, S.H., Song, Y.K., Han, G.M., Shim, W.J, 2019. Spatiotemporal distribution and annual load of microplastics in the Nakdong River, South Korea. Water Res. 160, 228–237.
Frank, Y.A., Vorobiev, E.D., Vorobiev, D.S., Trifonov, A.A., Antsiferov, D.V., Soliman Hunter, T., Wilson, S.P., Strezov, V., 2021. Preliminary Screening for Microplastic Concentrations in the Surface Water of the Ob and Tom Rivers in Siberia, Russia. Sustainability 13 (1), 80.
Gong, J., Xie, P., 2020. Research progress in sources, analytical methods, eco-environmental effects, and control measures of microplastics. Chemosphere 254, 126790–126791.
Grbic, J., Helm, P., Athey, S., Rochman, C.M, 2020. Microplastics entering northwestern Lake Ontario are diverse and linked to urban sources. Water Res. 174, 115623–115624.
Hendrickson, E., Minor, E.C., Schreiner, K., 2018. Microplastic abundance and composition in western lake superior as determined via microscopy, Pyr-GC/MS, and FTIR. Environ. Sci. Technol. 52 (4), 1787–1796.
Hernandez, E., Nowack, B., Mitrano, D.M, 2017. Polyester textiles as a source of microplastics from households: a mechanistic study to understand microfiber release during washing. Environ. Sci. Technol. 51 (12), 7036–7046.
Hua, Z., Li, L., Na, J., 2021. Microplastics detected in intestinal tissue of a pig raised near a sludge dump site: a pilot study. China J. Public Health 37 (3), 455–460.
Hurley, R., Woodward, J., Rothwell, J.J, 2018. Microplastic contamination of river beds significantly reduced by catchment-wide flooding. Nat. Geosci. 11 (4), 251.
Klein, M., Fischer, E.K, 2019. Microplastic abundance in atmospheric deposition within the Metropolitan area of Hamburg, Germany. Sci. Total Environ. 685, 96–103.
Klein, S., Worch, E., Knepper, T.P, 2015. Occurrence and spatial distribution of microplastics in river shore sediments of the Rhine-main area in Germany. Environ. Sci. Technol. 49 (10), 6070–6076.
Koelmans, A.A., Nor, N.H.M., Hermsen, E., Kooi, M., Mintenig, S.M., De France, J., 2019. Microplastics in freshwaters and drinking water: critical review and assessment of data quality. Water Res. 155, 410–422.
Leslie, H.A., Brandsma, S.H., van Velzen, M.J.M., Vethaak, A.D, 2017. Microplastics en route: field measurements in the Dutch river delta and Amsterdam canals, wastewater treatment plants, North Sea sediments and biota. Environ. Int. 101, 133–142.

Li, L., Geng, S., Wu, C., Song, K., Sun, F., Visvanathan, C., Xie, F., Wang, Q., 2019. Microplastics contamination in different trophic state lakes along the middle and lower reaches of Yangtze River Basin. Environ. Pollut. 254.
Li, Q., Zeng, A., Jiang, X., Gu, X., 2021. Are microplastics correlated to phthalates in facility agriculture soil? J. Hazard. Mater. 412.
Lin, L., Zuo, L.Z., Peng, J.P., Cai, L.Q., Fok, L., Yan, Y., Li, H.X., Xu, X.R, 2018. Occurrence and distribution of microplastics in an urban river: a case study in the Pearl River along Guangzhou City, China. Sci. Total Environ. 644, 375–381.
Long, Z., Pan, Z., Wang, W., Ren, J., Yu, X., Lin, L., Lin, H., Chen, H., Jin, X., 2019. Microplastic abundance, characteristics, and removal in wastewater treatment plants in a coastal city of China. Water Research 155, 255–265.
Mani, T., Primpke, S., Lorenz, C., Gerdts, G., Burkhardt-Holm, P., 2019. Microplastic pollution in benthic midstream sediments of the Rhine River. Environ. Sci. Technol. 53 (10), 6053–6062.
Mao, Y., Li, H., Gu, W., Yang, G., Liu, Y. and He, Q. 2020. Distribution and characteristics of microplastics in the Yulin River, China: Role of environmental and spatial factors. Environmental Pollution 265(Part A), 115033.
Masura, J. 2015. Laboratory methods for the analysis of microplastics inthe marine environment: recommendations for quantifying synthetic particles inwaters and sediments. NOAA Marine.
Mbedzi, R., Cuthbert, R.N., Wasserman, R.J., Murungweni, F.M., Dalu, T., 2020. Spatiotemporal variation in microplastic contamination along a subtropical reservoir shoreline. Environ. Sci. Pollut. Res. Int. 27, 23880–23887.
Mintenig, S.M., Int-Veen, I., Loeder, M.G.J., Primpke, S., Gerdts, G., 2017. Identification of microplastic in effluents of waste water treatment plants using focal plane array-based micro-Fourier-transform infrared imaging. Water Research 108, 365–372.
Mintenig, S.M., Kooi, M., Erich, M.W., Primpke, S., Redondo-Hasselerharm, P.E., Dekker, S.C., Koelmans, A.A., van Wezel, A.P., 2020. A systems approach to understand microplastic occurrence and variability in Dutch riverine surface waters. Water Res. 176, 115723–115724.
Murphy, F., Ewins, C., Carbonnier, F., Quinn, B., 2016. Wastewater Treatment Works (WwTW) as a Source of Microplastics in the Aquatic Environment. Environmental Science & Technology 50 (11), 5800–5808.
Napper, I.E., Baroth, A., Barrett, A.C., Bhola, S., Chowdhury, G.W., Davies, B.F.R., Duncan, E.M., Kumar, S., Nelms, S.E., Hasan Niloy, M.N., Nishat, B., Maddalene, T., Thompson, R.C., Koldewey, H., 2021. The abundance and characteristics of microplastics in surface water in the transboundary Ganges River. Environ. Pollut. 274, 116348–116349 (Barking, Essex: 1987).
Nocon, W., Moraczewska-Majkut, K., Wisniowska, E., 2020. Microplastics upstream and downstream dam-reservoirs. Desalin. Water Treat 199, 263–272.
Park, H.-J., Oh, M.-J., Kim, P.-G., Kim, G., Jeong, D.-H., Ju, B.-K., Lee, W.-S., Chung, H.-M., Kang, H.-J., Kwon, J.-H., 2020. National Reconnaissance Survey of Microplastics in Municipal Wastewater Treatment Plants in Korea. Environmental Science & Technology 54 (3), 1503–1512.
Peng, G., Xu, P., Zhu, B., Bai, M., Li, D., 2018. Microplastics in freshwater river sediments in Shanghai, China: a case study of risk assessment in mega-cities. Environ. Pollut. 234, 448–456.
Ribeiro, F., Okoffo, E.D., O'Brien, J.W., Fraissinet-Tachet, S., O'Brien, S., Gallen, M., Samanipour, S., Kaserzon, S., Mueller, J.F., Galloway, T., Thomas, K.V, 2020. Quantitative analysis of selected plastics in high-commercial-value australian seafood by pyrolysis gas chromatography mass spectrometry. Environ. Sci. Technol. 54 (15), 9408–9417.
Rodrigues, M.O., Abrantes, N., Goncalves, F.J.M., Nogueira, H., Marques, J.C., Goncalves, A.M.M, 2018. Spatial and temporal distribution of microplastics in water and sediments of a freshwater system (Antua River, Portugal). Sci. Total Environ. 633, 1549–1559.
Sait, S.T.L., Sorensen, L., Kubowicz, S., Vike-Jonas, K., Gonzalez, S.V., Asimakopoulos, A. G., Booth, A.M., 2020. Microplastic fibres from synthetic textiles: environmental degradation and additive chemical content. Environ. Pollut. 268, 115745–115746 (Barking, Essex: 1987)Pt B.
Samandra, S., Johnston, J.M., Jaeger, J.E., Symons, B., Xie, S., Currell, M., Ellis, A.V., Clarke, B.O, 2022. Microplastic contamination of an unconfined groundwater aquifer in Victoria, Australia. Sci. Total Environ. 802.
Scircle, A., Cizdziel, J.V., Tisinger, L., Anumol, T., Robey, D., 2020. Occurrence of microplastic pollution at oyster reefs and other coastal sites in the mississippi sound, USA: impacts of freshwater inflows from flooding. Toxics 8 (2).
Simon, M., van Alst, N., Vollertsen, J., 2018. Quantification of microplastic mass and removal rates at wastewater treatment plants applying Focal Plane Array (FPA)-based Fourier Transform Infrared (FT-IR) imaging. Water Res. 142, 1–9.
Su, L., Xue, Y., Li, L., Yang, D., Kolandhasamy, P., Li, D., Shi, H., 2016. Microplastics in Taihu Lake, China. Environ. Pollut. 216, 711–719.
Sun, J., Dai, X., Wang, Q., van Loosdrecht, M.C.M., Ni, B.-J, 2019. Microplastics in wastewater treatment plants: detection, occurrence and removal. Water Res. 152, 21–37.
Sutherland, W.J., Clout, M., Cote, I.M., Daszak, P., Depledge, M.H., Fellman, L., Fleishman, E., Garthwaite, R., Gibbons, D.W., De Lurio, J., Impey, A.J., Lickorish, F., Lindenmayer, D., Madgwick, J., Margerison, C., Maynard, T., Peck, L.S., Pretty, J., Prior, S., Redford, K.H., Scharlemann, J.P.W., Spalding, M., Watkinson, A.R, 2010. A horizon scan of global conservation issues for 2010. Trends Ecol. Evol. (Amst.) 25 (1), 1–7.
Tang, N., Liu, X., Xing, W., 2020. Microplastics in wastewater treatment plants of Wuhan, Central China: Abundance, removal, and potential source in household wastewater. Science of The Total Environment 745, 141026.
Thompson, R.C., Olsen, Y., Mitchell, R.P., Davis, A., Rowland, S.J., John, A.W.G., McGonigle, D., Russell, A.E, 2004. Lost at sea: where is all the plastic? Science 304 (5672), 838–839.
Wang, F., Wang, B., Duan, L., Zhang, Y., Zhou, Y., Sui, Q., Xu, D., Qu, H., Yu, G., 2020. Occurrence and distribution of microplastics in domestic, industrial, agricultural and aquacultural wastewater sources: a case study in Changzhou, China. Water Res. 182.
Wang, T., Li, B., Zou, X., Wang, Y., Li, Y., Xu, Y., Mao, L., Zhang, C., Yu, W., 2019. Emission of primary microplastics in mainland China: invisible but not negligible. Water Res. 162, 214–224.
Wong, G., Lowemark, L., Kunz, A., 2020. Microplastic pollution of the Tamsui River and its tributaries in northern Taiwan: spatial heterogeneity and correlation with precipitation. Environ. Pollut. 260.
Wright, S.L., Kelly, F.J., 2017. Plastic and human health: a micro issue? Environ. Sci. Technol. 51 (12), 6634–6647.
Wu, X., Pan, J., Li, M., Li, Y., Bartlam, M., Wang, Y., 2019. Selective enrichment of bacterial pathogens by microplastic biofilm. Water Res. 165.
Xiong, X., Wu, C., Elser, J.J., Mei, Z., Hao, Y., 2019. Occurrence and fate of microplastic debris in middle and lower reaches of the Yangtze River - From inland to the sea. Sci. Total Environ. 659, 66–73.
Zhang, L., Xie, Y., Zhong, S., Liu, J., Qin, Y., Gao, P., 2021. Microplastics in freshwater and wild fishes from Lijiang River in Guangxi, Southwest China. Sci. Total Environ. 755.
Zhou, Y.F., He, G., Jiang, X.L., Yao, L.G., Ouyang, L., Liu, X.Y., Liu, W.Z., Liu, Y., 2021. Microplastic contamination is ubiquitous in riparian soils and strongly related to elevation, precipitation and population density. J. Hazard. Mater. 411.